MEMS Reference Shelf

Cenk Acar
Andrei Shkel

MEMS Vibratory Gyroscopes

Structural Approaches to Improve Robustness

Springer

MEMS Vibratory Gyroscopes

Structural Approaches to Improve Robustness

MEMS Reference Shelf

Series Editors:

Stephen D. Senturia
Professor of Electrical Engineering, Emeritus
Massachusetts Institute of Technology
Cambridge, Massachusetts

Roger T. Howe
Department of Electrical Engineering
Stanford University
Stanford, California

Antonio J. Ricco
Small Satellite Division
NASA Ames Research Center
Moffett Field, California

MEMS Vibratory Gyroscopes Structural Approaches to Improve Robustness
Cenk Acar and Andrei Shkel
ISBN: 978-0-387-09535-6

BioNanoFluidic MEMS
Peter Hesketh, ed.
ISBN 978-0-387-46281-3

Microfluidic Technologies for Miniaturized Analysis Systems
Edited by Steffen Hardt and Friedhelm Schöenfeld, eds.
ISBN 978-0-387-28597-9

Forthcoming Titles

Self-assembly from Nano to Milli Scales
Karl F. Böhringer
ISBN 978-0-387-30062-7

Photonic Microsystems
Olav Solgaard
ISBN 978-0-387-29022-5

Micro Electro Mechanical Systems: A Design Approach
Kanakasabapathi Subramanian
ISBN 978-0-387-32476-0

Experimental Characterization Techniques for Micro-Nanoscale Devices
Kimberly L. Turner and Peter G. Hartwell
ISBN 978-0-387-30862-3

Microelectroacoustics: Sensing and Actuation
Mark Sheplak and Peter V. Loeppert
ISBN 978-0-387-32471-5

Inertial Microsensors
Andrei M. Shkel
ISBN 978-0-387-35540-5

Cenk Acar and Andrei Shkel

MEMS Vibratory Gyroscopes

Structural Approaches to Improve Robustness

Springer

Cenk Acar
Systron Donner Automotive
2700 Systron Drive
Concord, CA 94518-1399

Andrei Shkel
University of California, Irvine
Dept. of Mechanical and Aerospace Engineering
4200 Engineering Gateway Building
Irvine, CA 92697-3975

Library of Congress Control Number: 2008932165

ISBN 978-0-387-09535-6 e-ISBN 978-0-387-09536-3

Printed on acid-free paper.

Printed on acid-free paper.

9 8 7 6 5 4 3 2 1

springer.com

To my beloved wife Şebnem Acar, and my dear parents.

Preface

Merging electrical and mechanical systems at a micro scale, Microelectromechanical Systems (MEMS) technology has revolutionized inertial sensors. Since the first demonstration of a micromachined gyroscope by the Draper Laboratory in 1991, various micromachined gyroscope designs fabricated in surface micromachining, bulk micromachining, hybrid surface-bulk micromachining technologies or alternative fabrication techniques have been reported. Inspired by the promising success of micromachined accelerometers in the same era, extensive research efforts towards commercial micromachined gyroscopes led to several innovative gyroscope topologies, fabrication and integration approaches, and detection techniques. Consequently, vibratory micromachined gyroscopes that utilize vibrating elements to induce and detect Coriolis force have been effectively implemented and demonstrated in various micromachining-based batch fabrication processes. However, achieving robustness against fabrication variations and environmental fluctuations still remains as one of the greatest challenges in commercialization and high-volume production of micromachined vibratory rate gyroscopes.

The limitations of the photolithography-based micromachining technologies define the upper-bound on the performance and robustness of micromachined gyroscopes. Conventional gyroscope designs based on matching or near-matching the drive and sense mode resonant frequencies are quite sensitive to variations in oscillatory system parameters. Thus, producing stable and reliable vibratory micromachined gyroscopes have proven to be extremely challenging, primarily due to the high sensitivity of the dynamical system response to fabrication and environmental variations.

In the first part of this book, we review the Coriolis effect and angular rate sensors, and fundamental operational principles of micromachined vibratory gyroscopes. We review basic mechanical and electrical design and implementation practices, system-level architectures, and common fabrication methods utilized for MEMS gyroscopes and inertial sensors in general. We also discuss electrical and mechanical parasitic effects such as structural imperfections, and analyze their impact on the sensing element dynamics.

In the second part, we review recent results of the study on design concepts that explore the possibility of shifting the complexity from the control electronics to the structural design of the gyroscope dynamical system. The fundamental approach is to develop structural designs and dynamical systems for micromachined gyroscopes that provide inherent robustness against structural and environmental parameter variations. In this context, we primarily focus on obtaining a gain and phase stable region in the drive and sense-mode frequency responses in order to achieve overall system robustness. Operating in the stable drive and sense frequency regions provides improved bias stability, temperature stability, and immunity to environmental and fabrication variations. Toward this goal, two major design concepts are investigated: expanding the dynamic system design space by increasing the degree-of-freedom of the drive and sense mode oscillatory system, and utilizing an array of drive-mode oscillators with incrementally spaced resonant frequencies.

This book provides a solid foundation in the fundamental theory, design and implementation of micromachined vibratory rate gyroscopes, and introduces a new paradigm in MEMS gyroscope sensing element design, where disturbance-rejection capability is achieved by the mechanical system instead of active control and compensation strategies. The micromachined gyroscopes of this class are expected to lead to reliable, robust and high performance angular-rate sensors with low production costs and high yields, fitting into or enabling many applications in the aerospace/defense, automotive and consumer electronics markets.

June 2008 *Cenk Acar, Andrei Shkel*

Contents

Part I
Fundamentals of Micromachined Vibratory Gyroscopes

Chapter 1
Introduction

In this chapter, we present a brief overview of the Coriolis effect and angular rate sensors, micromachining and the MEMS technology, implementation of vibratory gyroscopes at the micro-scale, and a chronological survey of the prior work on micromachined gyroscopes.

1.1 The Coriolis Effect

The Coriolis effect, which defies common sense and intuition, has been observed but not fully understood for centuries. Found on many archaeological sites, the ancient toy spinning top (Figure 1.1) is an excellent example that the Coriolis effect was part of the daily life over three thousand years before Gaspard Gustave Coriolis first derived the mathematical expression of the Coriolis force in his paper *"Mémoire sur les équations du mouvement relatif des systémes de corps"* [1] investigating moving particles in rotating systems in 1835.

Fig. 1.1 A wooden decorated spinning top from the 14th century BC found in the tomb of Tutankhamun, currently at the Egyptian Museum. One of the most beloved toys of Egyptian children in ancient times, the spinning top relies on the Coriolis effect to spin upright and slowly starts precessing as it loses angular momentum [40].

The Coriolis effect arises from the fictitious Coriolis force, which appears to act on an object only when the motion is observed in a rotating non-inertial reference frame. The Foucault pendulum (Figure 1.2) demonstrates this phenomenon very well: When a swinging pendulum attached to a rotating platform such as earth is observed by a stationary observer in space, the pendulum oscillates along a constant straight line. However, an observer on earth observes that the line of oscillation precesses. In the dynamics with respect to the rotating frame, the precession of the pendulum can only be explained by including the Coriolis force in the equations of motion.

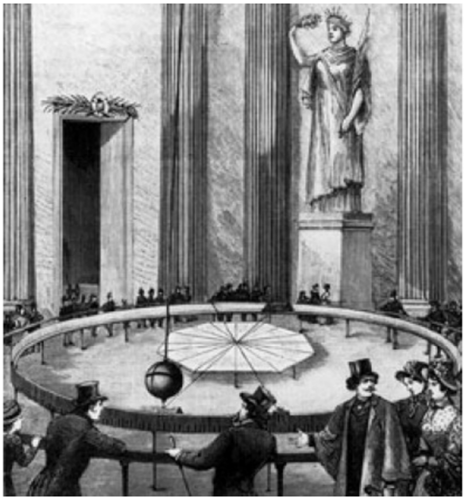

Fig. 1.2 The Foucault pendulum, invented by Jean Bernard Léon Foucault in 1851 as an experiment to demonstrate the rotation of the earth. The swinging direction of the pendulum rotates with time at a rate proportional to the sine of the latitude due to earth's rotation [41].

1.2 Gyroscopes

In simplest terms, gyroscope is the sensor that measures the rate of rotation of an object. The name "gyroscope" originated from Léon Foucault, combining the Greek word "skopeein" meaning to see and the Greek word "gyros" meaning rotation, during his experiments to measure the rotation of the Earth.

The earliest gyroscopes, such as the Sperry gyroscope, and many modern gyroscopes utilize a rotating momentum wheel attached to a gimbal structure. However, rotating wheel gyroscopes came with many disadvantages, primarily concerning bearing friction and wear. Vibrating gyroscopes, such as the Hemispherical Resonator Gyroscope (HRG) and Tuning-Fork Gyroscopes presented an effective solution to the bearing problems by eliminating rotating parts.

Alternative high-performance technologies such as the Fiber-Optic Gyroscope (FOG) and Ring Laser Gyroscope (RLG) based on the Sagnac effect have also been developed. By eliminating virtually all mechanical limitations such as vibration and shock sensitivity and friction, these optical gyroscopes found many high-end applications despite their high costs.

Fig. 1.3 One of the first examples of the gyrocompass, developed in the early 1800s. The gyrocompass gained popularity, especially in steel ships, since steel blocked the ability of magnetic compasses to find magnetic north.

1.3 The MEMS Technology

As the name implies, Microelectromechanical Systems (MEMS) is the technology that combines electrical and mechanical systems at a micro scale. Practically, any device fabricated using photo-lithography based techniques with micrometer ($1\mu\text{m} = 10^{-6}\text{m}$) scale features that utilizes both electrical and mechanical functions could be considered MEMS.

Evolved from the semiconductor fabrication technologies, the most striking feature of the MEMS technology is that it allows building moving micro-structures on a substrate. With this capability, extremely complex mechanical and electrical systems can be created. Masses, flexures, actuators, detectors, levers, linkages, gears, dampers, and many other functional building blocks can be combined to build complete sophisticated systems on a chip. Inertial sensors such as accelerometers and gyroscopes utilize this capability to its fullest.

Photolithography based pattern transfer methods and successive patterning of thin structural layers adapted from standard IC fabrication processes are the enabling technologies behind micromachining. By dramatically miniaturizing and batch processing complete electro-mechanical systems, substantial reductions in device size, weight and cost are achieved.

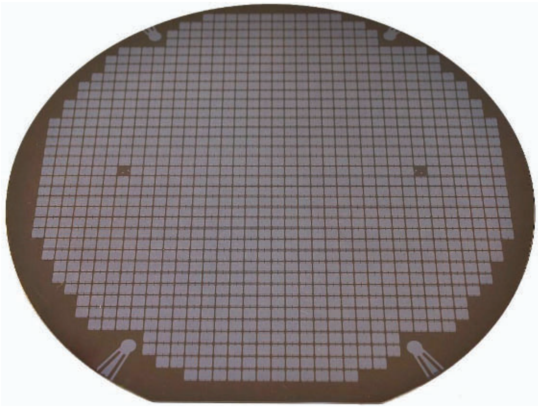

Fig. 1.4 A 150mm wafer from a gyroscope prototyping run. In a typical production process, it is common to have well over 2000 devices on a 150mm wafer.

1.4 Micromachined Vibratory Rate Gyroscopes

Even though an extensive variety of micromachined gyroscope designs and operation principles exist, majority of the reported micromachined gyroscopes use vibrating mechanical elements to sense angular rate. The concept of utilizing vibrating elements to induce and detect Coriolis force presents many advantages by involving no rotating parts that require bearings and eliminating friction and wear. That is the primary reason why vibratory gyroscopes have been successfully miniaturized by the use of micromachining processes, and have become an attractive alternative to their macro-scale counterparts.

The fundamental operation principle of micromachined vibratory gyroscopes relies on the sinusoidal Coriolis force induced due to the combination of vibration of a proof-mass and an orthogonal angular-rate input. The proof mass is generally suspended above the substrate by a suspension system consisting of flexible beams. The overall dynamical system is typically a two degrees-of-freedom (2-DOF) mass-spring-damper system, where the rotation-induced Coriolis force causes

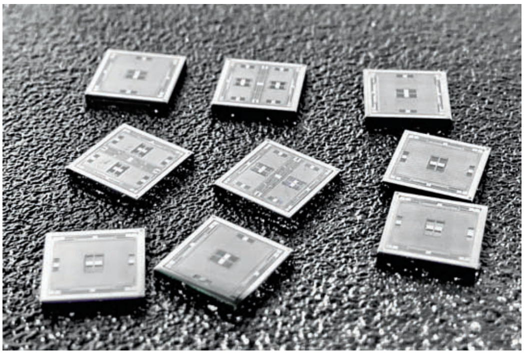

Fig. 1.5 Singulated micromachined gyroscope dice designed and fabricated at UCI Microsystems Laboratory. Courtesy of Alexander A. Trusov.

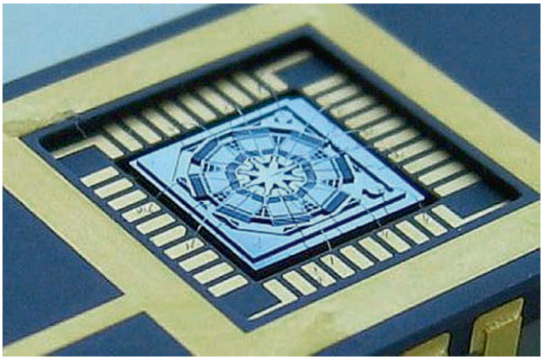

Fig. 1.6 A packaged MEMS gyroscope chip. The three-dimensional micro-scale structure is formed out of single-crystal silicon on a silicon substrate, complete with moving proof-masses, suspension beams, actuators and detectors.

energy transfer to the sense-mode proportional to the angular rate input. In most of the reported micromachined vibratory rate gyroscopes, the proof mass is driven into resonance in the drive direction by an external sinusoidal electrostatic or electromagnetic force. When the gyroscope is subjected to an angular rotation, a sinusoidal Coriolis force at the driving frequency is induced in the direction orthogonal to both the drive-mode oscillation and the angular rate axis.

Ideally, it is desired to utilize resonance in both the drive and the sense modes in order to attain the maximum possible response gain and sensitivity. This is typically achieved by designing and if needed tuning the drive and sense resonant frequencies to match. Alternatively, the sense-mode is designed to be slightly shifted from the drive-mode to improve robustness and thermal stability, while intentionally sacrificing gain and sensitivity.

Even though increasing the spacing between the drive and sense frequencies reduces the impact of variations in oscillatory system parameters that shift the natural

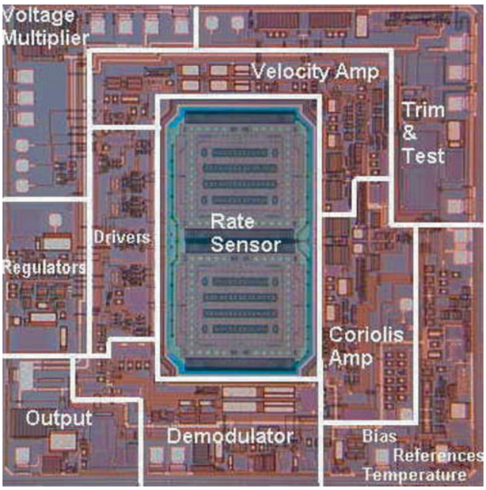

Fig. 1.7 The iMEMS ADXRS angular rate sensor by Analog Devices is an excellent example of a micromachined vibratory gyroscope, which integrates the angular rate sensing element and signal processing electronics on the same die. Courtesy of Analog Devices.

frequencies and damping values, the resulting errors still require compensation by advanced control and signal processing architectures.

1.5 Applications of MEMS Gyroscopes

As their performance keeps constantly improving in time, micromachined gyroscopes are becoming a viable alternative to expensive and bulky conventional inertial sensors. High-performance angular rate sensors such as precision fiber-optic gyroscopes, ring laser gyroscopes, and conventional rotating wheel gyroscopes are usually too expensive and too large for use in most emerging applications. With micromachining processes that allow batch production of micro-electro-mechanical systems on a chip similar to integrated circuits, unit costs unimaginable in any other technology are achieved. Moreover, advances in the fabrication techniques that allow electronics to be integrated on the same silicon chip together with the mechanical sensor elements provide an unmatched integration capability. Consequently, miniaturization of vibratory gyroscopes with innovative micro-fabrication processes and gyroscope designs is already becoming an attractive solution to current inertial sensing market needs, and even opening new market opportunities.

With their dramatically reduced cost, size, and weight, MEMS gyroscopes potentially have a wide application spectrum in the aerospace industry, military, automotive and consumer electronics markets. The automotive industry applications are diverse, including advanced automotive safety systems such as electronic stability control (ESC), high performance navigation and guidance systems, ride stabilization, roll-over detection and prevention, and next generation airbag and brake systems. A wide range of consumer electronics applications with very high volumes include image stabilization in digital cameras and camcorders, virtual reality products, inertial pointing devices, and computer gaming industry. Miniaturization of gyroscopes also enable higher-end applications including micro-satellites, micro-robotics, and even implantable devices to cure vestibular disorders.

1.6 Gyroscope Performance Specifications

The specifications and test procedures for rate gyroscopes are outlined in the *IEEE Standard Specification Format Guide and Test Procedure for Coriolis Vibratory Gyros* [2]. The following is a summary of important specifications and definitions from *IEEE Standard for Inertial Sensor Terminology* [3].

Scale factor:

The ratio of a change in output to a change in the input intended to be measured, typically specified in mV/°/sec, and evaluated as the slope of the least squares straight line fit to input-output data. Scale factor error specifications include:

Linearity error: The deviation of the output from a least-squares linear fit of the input-output data. It is generally expressed as a percentage of full scale, or percent of output.

Nonlinearity: The systematic deviation from the straight line that defines the nominal input-output relationship.

Scale factor temperature and acceleration sensitivity: The change in scale factor resulting from a change in steady state operating temperature and a constant acceleration.

Asymmetry error: The difference between the scale factor measured with positive input and that measured with negative input, specified as a fraction of the scale factor measured over the input range.

Scale factor stability: The variation in scale factor over a specified time of continuous operation. Ambient temperature, power supply and additional factors pertinent to the particular application should be specified.

Bias (zero rate output):

The average over a specified time of gyro output measured at specified operating conditions that has no correlation with input rotation. Bias is typically expressed in °/sec or °/hr. The zero-rate output drift rate specifications include:

Random drift rate: The random time-varying component of drift rate. Random drift rate is usually defined in terms of the Allan variance components:

a) Angle Random Walk: The angular error buildup with time that is due to white noise in angular rate, typically expressed in $°/\sqrt{\text{hr}}$ or $°/\text{s}/\sqrt{\text{hr}}$.

b) Bias Instability: The random variation in bias as computed over specified finite sample time and averaging time intervals, characterized by a $1/f$ power spectral density, typically expressed in °/hr.

c) Rate Random Walk: The drift rate error buildup with time that is due to white noise in angular acceleration, typically expressed in $°/\text{hr}/\sqrt{\text{hr}}$.

Environmentally sensitive drift rate: Components of drift rate dependent on environmental parameters, including acceleration sensitivity, temperature sensitivity, temperature gradient sensitivity, temperature hysteresis and vibration sensitivity.

Operating range (input rate limits):

Range of positive and negative angular rates that can be detected without saturation.

Resolution:

The largest value of the minimum change in input, for inputs greater than the noise level, that produces a change in output equal to some specified percentage (at least 50%) of the change in output expected using the nominal scale factor.

Bandwidth:

The range of frequency of the angular rate input that the gyroscope can detect. Typically specified as the cutoff frequency coinciding to the -3dB point. Alternatively, the frequency response or transfer function could be specified.

Turn-on time:
The time from the initial application of power until a sensor produces a specified useful output, though not necessarily at the accuracy of full specification performance.

Linear and angular vibration sensitivity:
The ratio of the change in output due to linear and angular vibration about a sensor axis to the amplitude of the angular vibration causing it.

Shock resistance:
Maximum shock that the operating or non-operating device can endure without failure, and conform to all performance requirements after exposure. Pulse duration and shape have to be specified. Full recovery time after exposure can also be specified.

Reliability requirements such as operating life, operating temperature range, thermal shock, thermal cycling, humidity, electrostatic discharge (ESD) immunity, and electromagnetic emissions and susceptibilities are also typically specified in many applications.

1.7 A Survey of Prior Work on MEMS Gyroscopes

Since the first demonstration of a micromachined gyroscope by the Draper Laboratory in 1991 [6], various micromachined gyroscope designs fabricated in a variety of processes including surface, bulk and hybrid surface-bulk micromachining technologies or alternative fabrication techniques have been reported in the literature. The development of miniaturized piezoelectric gyroscopes, for example the quartz tuning-fork by Systron Donner [7] and the fused-quartz HRG by Delco [8], date back to the early 1980's. Incompatibility of quartz devices with IC fabrication technologies and the know-how generated from micromachined accelerometers in the same era led to several successful academic and commercial silicon-based microgyroscopes over the following decades.

1.7.0.1 Important Development Milestones

The evolution of the design and performance of silicon micromachined gyroscopes is better understood by investigating the important development milestones in chronological order:

- Draper Laboratory reported the first micromachined gyroscope in 1991, utilizing a double-gimbal single crystal silicon structure suspended by torsional flexures; and demonstrated $4^\circ/\mathrm{s}/\sqrt{\mathrm{Hz}}$ resolution at 60Hz bandwidth [6].
- In 1993, Draper Laboratory reported their next generation silicon-on-glass tuning fork gyroscope with $1^\circ/\mathrm{s}/\sqrt{\mathrm{Hz}}$ resolution. The glass substrate aimed to minimize stray capacitance. The tuning fork proof masses were driven out of-phase

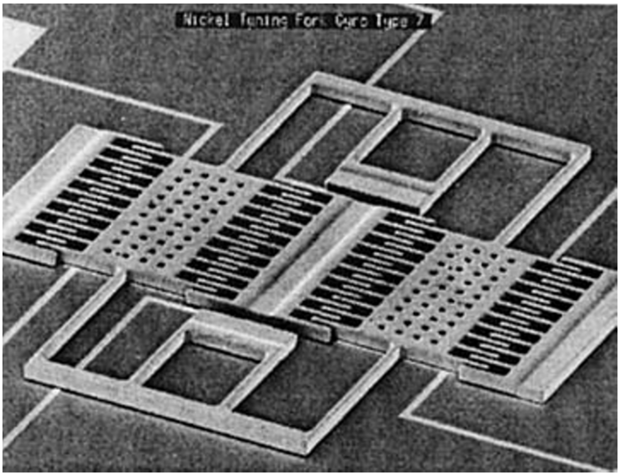

Fig. 1.8 The scanning electron micrograph image of the first working prototype tuning fork gyroscope from the Draper Laboratory. The device utilizes single-crystal silicon as the structural material, fabricated with a dissolved wafer process [9].

electrostatically with comb-drives, and the sense resoponse in the out-of-plane rocking mode was detected [9].

- University of Michigan developed a vibrating ring gyroscope with $0.5^\circ/\mathrm{s}/\sqrt{\mathrm{Hz}}$ resolution in 1994, fabricated by metal electroforming [10]. The in-plane elliptically shaped primary mode of the ring was electrostatically excited, and the transfer of energy to the secondary flexural mode due to the Coriolis force was detected.
- British Aerospace Systems reported a single crystal silicon ring gyroscope in 1994. The sensor structure was formed on glass substrate by deep dry etching of a 100μm silicon wafer. Silicon Sensing Systems and Sumitomo Precision Products have commercialized this sensor with a resolution of $0.5^\circ/\mathrm{s}/\sqrt{\mathrm{Hz}}$ over a 100Hz bandwidth [11].
- Murata developed a lateral axis (x or y) surface-micromachined polysilicon gyroscope in 1995. The sensing electrodes underneath the perforated polysilicon resonator of the gyroscope were formed by diffusing phosphorus into the substrate. A resolution of $2^\circ/\mathrm{s}/\sqrt{\mathrm{Hz}}$ was reported [12].
- Berkeley Sensor and Actuator Center (BASC) utilized the integrated surface micromachining process iMEMS by Analog Devices Inc. to develop an integrated z-axis gyroscope in 1996 [13], and an x-y dual axis gyroscope in 1997 [14]. The z-axis gyroscope with a resolution of $1^\circ/\mathrm{s}/\sqrt{\mathrm{Hz}}$ employed a single proof-mass driven into resonance in-plane, and sensitive to Coriolis motion in the in-plane orthogonal direction. Drive and sense modes were electrostatically tuned to match, and the quadrature error due to structural imperfections were compensated electrostatically. The x-y dual axis gyroscope with a 2μm thick polysilicon rotor

disc utilized torsional drive-mode excitation and two orthogonal torsional sense modes to achieve a resolution of $0.24^\circ/\mathrm{s}/\sqrt{\mathrm{Hz}}$.

- In 1997, Robert Bosch Gmbh. reported z-axis micromachined tuning-fork gyroscope design that utilizes electromagnetic drive and capacitive sensing for automotive applications, with a resolution of $0.4^\circ/\mathrm{s}/\sqrt{\mathrm{Hz}}$ [15]. Through the use of a permanent magnet inside the sensor package, drive-mode amplitudes in the order of 50μm were achieved.
- Jet Propulsion Laboratory (JPL) developed a bulk micromachined clover-leaf shaped gyroscope in 1997 together with UCLA. The device had a metal post epoxied inside a hole on the silicon resonator to increase the rotational inertia of the sensing element. A resolution of $70^\circ/\mathrm{hr}/\sqrt{\mathrm{Hz}}$ was demonstrated [16].
- Delphi reported a vibratory ring gyroscope with an electroplated metal ring structure in 1997. The ring was built on top of CMOS chips, and suspended by semicircular rings. The measured noise floor was $0.1^\circ/\mathrm{s}/\sqrt{\mathrm{Hz}}$ with 25 Hz bandwidth [17].
- In 1997, Samsung presented a 7.5μm thick low-pressure chemical vapor deposited polysilicon gyroscope with 0.3μm polysilicon lower sensing electrodes [18], similar to Murata's sensor. The device exhibited $0.1^\circ/\mathrm{s}/\sqrt{\mathrm{Hz}}$ resolution with vacuum-packaging. An in-plane device with four fish-hook spring suspension was also demonstrated with the same resolution [19].
- Daimler Benz reported an SOI-based bulk-micromachined tuning-fork gyroscope with piezoelectric drive and piezoresistive detection in 1997. Piezoelectric aluminum nitride was deposited on one of the tines as the actuator layer, and the rotation induced shear stress in the step of the tuning fork was piezoresistively detected [20].
- Allied Signal developed bulk-micromachined single crystal silicon sensors in 1998, and demonstrated a resolution of $18^\circ/\mathrm{hr}/\sqrt{\mathrm{Hz}}$ at 100Hz bandwidth [21].
- Draper Laboratories reported a 10μm thick surface-micromachined polysilicon gyroscope in 1998. The resolution was improved to $10^\circ/\mathrm{hr}/\sqrt{\mathrm{Hz}}$ at 60Hz bandwidth in 1993, with temperature compensation and better control techniques [22].
- In 1999, Murata developed a DRIE-based 50μm thick bulk micromachined single crystal silicon gyroscope with independent beams for drive and detection modes, which aimed to minimize undesired coupling between the drive and sense modes. A resolution of $0.07^\circ/\mathrm{s}/\sqrt{\mathrm{Hz}}$ was demonstrated at 10Hz bandwidth [23].
- Robert Bosch Gmbh. developed a surface micromachined gyroscope with thick polysilicon structural layer in 1999. The device with 12μm thick polysilicon layer demonstrated a $0.4^\circ/\mathrm{s}/\sqrt{\mathrm{Hz}}$ resolution at 100Hz bandwidth [24].
- Samsung demonstrated a wafer-level vacuum packaged 40μm thick bulk micromachined single crystal silicon sensor with mode decoupling in 2000, and reported a resolution of $0.013^\circ/\mathrm{s}/\sqrt{\mathrm{Hz}}$ [25].
- Seoul National University reported a hybrid surface-bulk micromachining process in 2000. The device with 40μm thick single crystal silicon demonstrated a resolution of $9^\circ/\mathrm{hr}/\sqrt{\mathrm{Hz}}$ at 100Hz bandwidth [26].
- In 2000, a z-axis vibratory gyroscope with digital output was developed at BSAC, utilizing the CMOS-compatible IMEMS process by Sandia National Laborato-

ries. Parallel-plate electrostatic actuation provided low actuation voltages with limited drive-mode amplitude. $3°/s/\sqrt{Hz}$ resolution was demonstrated at atmospheric pressure [27].

- Carnegie-Mellon University demonstrated both lateral-axis [28] and z-axis [29] integrated gyroscopes with noise floor of about $0.5°/s/\sqrt{Hz}$ using a maskless post-CMOS micromachining process in 2001. The lateral-axis gyroscope with 5 μm thick structure was fabricated by a thin-film CMOS process, starting with Agilent 0.5μm three-metal CMOS. Excessive curling was observed due to the residual stress and thermal expansion coefficient mismatch in the structure, and limited the device size. The 8μm thick z-axis integrated gyroscope was fabricated starting with UMC 0.18μm six copper layer CMOS.
- HSG-IMIT reported in 2002 a gyroscope with excellent structural decoupling of drive and sense modes, fabricated in the standard Bosch fabrication process featuring 10μm thick polysilicon structural layer. A resolution of $25°/hr/\sqrt{Hz}$ with 100Hz bandwidth was reported [30].
- Analog Devices Inc. developed a dual-resonator z-axis gyroscope in 2002, fabricated in the iMEMS process by ADI with a 4μm thick polysilicon structural layer. The device utilized two identical proof masses driven into resonance in opposite directions to reject external linear accelerations, and the differential output of the two Coriolis signals was detected. On-chip control and detection electronics provided self oscillation, phase control, demodulation and temperature compensation. This first commercial integrated micromachined gyroscope had a measured noise floor of $0.05°/s/\sqrt{Hz}$ at 100Hz bandwidth [31].
- An integrated micromachined gyroscope with resonant sensing was reported in 2002 by BSAC. Fabricated in the IMEMS process by Sandia National Laboratories, the device utilized frequency shift of double-ended tuning forks (DETF) due to the generated Coriolis force. A resolution of $0.3°/s/\sqrt{Hz}$ was demonstrated with the on-chip integrated electronics [32].
- In 2002, University of Michigan reported their 150μm thick bulk micromachined single crystal silicon vibrating ring gyroscope, with $10.4°/hr/\sqrt{Hz}$ resolution [33].
- In 2003, Carnegie-Mellon University demonstrated a DRIE CMOS-MEMS lateral axis gyroscope with a measured noise floor of $0.02°/s/\sqrt{Hz}$ at 5 Hz, fabricated by post-CMOS micromachining that uses interconnect metal layers to mask the structural etch steps. The device employs a combination of 1.8μm thin-film structures for springs with out-of-plane compliance and 60μm bulk silicon structures defined by DRIE for the proof mass and springs with out-of-plane stiffness, with on-chip CMOS circuitry. Complete etch removal of selective silicon regions provides electrical isolation of bulk silicon to obtain individually controllable comb fingers. Excessive curling is eliminated in the device, which was problematic in prior thin-film CMOS-MEMS gyroscopes [34].
- In 2004, Honeywell presented the experimental results on commercial development of MEMS vibratory gyroscopes [35], the adaptation of the tuning fork architecture originally developed by Draper's Laboratory. The demonstrated per-

formance of the gyro was 1440°/s operation range, less than 30°/hr bias in-run stability, and $0.05°/\sqrt{\text{hr}}$ angle random walk.

- In 2005, a bulk micromachined gyroscope with bandwidth of 58 Hz and 0.3°/hr bias stability tested in 10 mTorr pressure was presented by Seoul National University [36], however not enough details on design and testing conditions were given to independently verify the performance characteristics reported. There were no subsequent publications on the design supporting the data.
- In 2006, Microsystems Laboratory at UCIrvine introduced a design architecture of vibratory gyroscope with 1-DOF drive-mode and 2-DOF sense-mode [63]. The architecture provided a gain and phase stable operation region in the sense-mode frequency response to achieve inherent robustness at the sensing element level. The gyroscope exhibited a measured noise floor of $0.64°/\text{s}/\sqrt{\text{Hz}}$ at 50 Hz in atmospheric pressure with external discrete electronics.
- In 2007, Georgia Institute of Technology demonstrated a vibratory silicon gyroscope in a tuning fork arrangement to achieve 0.2°/hr bias drift with automatic mode-matching and sense-mode Quality factor of 36,000. The sense mode is automatically tuned down by the ASIC until the zero-rate output is maximized [37]. On the same device, 5.4°/hr bias drift and 1.5 Hz bandwidth for 2 Hz mode-mismatch and Quality factor of 10,000 at fixed temperature, and 0.96°/hr bias drift and 0.4bHz bandwidth for 0 Hz mode-mismatch and Quality factor of 40,000 were previously reported [38].
- In 2008, Microsystems Laboratory at UCIrvine improved the design architecture of structurally robust MEMS gyroscopes [151] and demonstrated high operational frequency devices (over 2.5kHz) and bandwidth over 250 Hz, with the uncompensated temperature coefficients of bias and scale factor of 313°/hr/°C and 351 ppm/°C, respectively. With off-chip detection electronics, the measured resolution was $0.09\ °/\text{s}/\sqrt{\text{Hz}}$ and the bias drift was 0.08 °/s.

1.8 The Robustness Challenge

The tolerancing capabilities of the current photolithography processes and microfabrication techniques are inadequate compared to the requirements for production of high-performance inertial sensors. The resulting inherent imperfections in the mechanical structure significantly limits the performance, stability, and robustness of MEMS gyroscopes [45, 61]. Thus, fabrication and commercialization of high-performance and reliable MEMS gyroscopes that require picometer-scale displacement measurements of a vibratory mass have proven to be extremely challenging [4,43].

In micromachined vibratory rate gyroscopes, the mode-matching requirement renders the system response very sensitive to variations in system parameters due to fabrication imperfections and fluctuations in operating conditions. Inevitable fabrication imperfections affect both the geometry and the material properties of MEMS devices [61], and shift the drive and sense-mode resonant frequencies. The dynamical system characteristics are observed to deviate drastically from the designed values and also from device to device, due to slight variations in photolithography steps, etching processes, deposition conditions or residual stresses. Process control becomes extremely critical to minimize die-to-die, wafer-to-wafer, and lot-to-lot variations.

Fluctuations in the temperature of the structure also perturb the dynamical system parameters due to the temperature dependence of Young's Modulus and thermally induced localized stresses. Temperature also drastically affects the damping and the Q factor in the drive and sense modes.

Extensive research has focused on design of symmetric suspensions and resonator systems that provide mode-matching and minimize temperature dependence [91, 92]. Various symmetric gyroscope designs based on enhancing performance by mode-matching have been reported. However, especially for lightly-damped devices, the requirement for mode-matching is well beyond fabrication tolerances; and none of the symmetric designs can provide the required degree of mode-matching without active tuning and closed-loop feedback control [46, 47]. Also the gain is affected significantly by fluctuations in damping conditions, which makes the device very vulnerable to any possible vacuum leak in the hermetic package seal or outgassing within the cavity.

Fabrication imperfections also introduce anisoelasticities due to extremely small imbalances in the gyroscope suspension. This results in mechanical interference between the modes and undesired mode coupling often much larger than the Coriolis motion. In order to suppress coupled oscillation and drift, various devices have been reported employing independent suspension beams for the drive and sense modes [85, 87–89, 91, 99].

Consequently, the mechanical sensing elements of micromachined gyroscopes are required to provide excellent performance, stability, and robustness to meet demanding specifications. Fabrication imperfections and variations, and fluctuations in the ambient temperature or pressure during the operation time of these devices introduce significant errors, which typically require electronic compensation. Closed-loop force-feedback implementations in the sense-mode are known to alleviate the sensitivity to frequency and damping variations, and increase the sensor bandwidth. However, a closed-loop sense-mode requires additional feedback electrodes, and increases the cost and complexity of both the MEMS device and the electronics. Thus, it is desirable to achieve inherent robustness at the sensing element to minimize compensation requirements.

1.9 Inherently Robust Systems

In recent years, a number of gyroscope designs with multiple proof-masses and different operation principles have been proposed to enhance performance and robustness of MEMS gyroscopes [49, 50, 54, 85, 87, 88, 99]. Most of these designs rely on constraining the oscillation degree-of-freedom of the driven mass to lie only in the drive direction. In these designs, either a part of the Coriolis Force induced on the driven mass is transferred to the sensing mass while suppressing the motion of the sensing mass in drive direction [49, 54, 85, 99]; or the drive direction oscillation of the driven mass is transferred to the sensing mass while the driven mass is not allowed to oscillate in the sense direction [50, 87, 88]. These designs are still virtually two degrees-of-freedom systems, however, they offer various advantages from the drive and sense mode decoupling and mode-matching points of view.

Multiple degrees-of-freedom resonators providing larger drive-direction amplitudes for improving the performance of vibratory MEMS devices have also been recently reported [52, 53, 56, 89, 93]. Two degrees-of-freedom oscillators utilizing mechanical amplification of motion for large oscillation amplitudes have been proposed, however, no results on integration of this oscillator system into MEMS gyroscopes have been indicated [52, 53, 93].

1.10 Overview

This book is organized in two parts. The first part reviews the fundamental operational principles of micromachined vibratory gyroscopes, mechanical sensing element design and practical implementation aspects, electrical design and system-level architectures for actuation and detection, basics of microfabrication methods used for MEMS gyroscopes, and test and characterization techniques. The second part reviews new dynamical systems and structural designs for micromachined gyroscopes, that will provide inherent robustness against structural and environmental parameter variations, and require less demanding active compensation schemes. The basic approach is to achieve a frequency response with an operating frequency region where the response gain and phase are stable, in contrast to a resonant conventional system.